STORAGE RING CROSS-SECTION MEASUREMENTS FOR ELECTRON IMPACT SINGLE AND DOUBLE IONIZATION OF Fe^{9+} AND SINGLE IONIZATION OF Fe^{10+}

M. HAHN[1], A. BECKER[2], M. GRIESER[2], C. KRANTZ[2], M. LESTINSKY[3], A. MÜLLER[4], O. NOVOTNÝ[1], R. REPNOW[3],
S. SCHIPPERS[4], K. SPRUCK[4], A. WOLF[2], AND D. W. SAVIN[1]
[1] Columbia Astrophysics Laboratory, Columbia University, 550 West 120th Street, New York, NY 10027, USA
[2] Max-Planck-Institut für Kernphysik, Saupfercheckweg 1, D-69117 Heidelberg, Germany
[3] GSI Helmholtzzentrum für Schwerionenforschung, Planckstr. 1, D-64291 Darmstadt, Germany
[4] Institut für Atom- und Molekülphysik, Justus-Liebig-Universität Giessen, Leihgesterner Weg 217, D-35392 Giessen, Germany

ABSTRACT

We have measured electron impact ionization from the ground state of Fe^{9+} and Fe^{10+} over the relative electron–ion collision energy ranges 200–1900 eV and 250–1800 eV, respectively. The ions were confined in an ion storage ring long enough for essentially all metastable levels to radiatively relax to the ground state. For single ionization, we find a number of discrepancies between the existing theoretical cross sections and our results. The calculations appear to neglect some excitation-autoionization (EA) channels, particularly from $n = 3$ to n' excitations, which are important near threshold, and those from $n = 2 \rightarrow 3$ excitations, which contribute at about 650 eV. Conversely, at higher energies the calculations appear to overestimate the importance of EA channels due to excitation into levels where $n \geqslant 4$. The resulting experimental rate coefficients agree with the most recent theory for Fe^{9+} to within 16% and for Fe^{10+} to within 19% at temperatures where these ions are predicted to form in collisional ionization equilibrium. We have also measured double ionization of Fe^{9+} forming Fe^{11+} in the energy range 450–3000 eV and found that although there is an appreciable cross section for direct double ionization, the dominant mechanism appears to be through direct ionization of an inner shell electron producing an excited state that subsequently stabilizes through autoionization.

Key words: atomic data – atomic processes

Online-only material: machine-readable tables
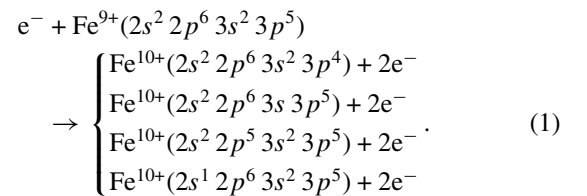
1. INTRODUCTION

Accurate cross-section data for electron impact ionization (EII) are needed to interpret the spectra of collisionally ionized plasmas, such as those formed in stellar coronae, supernova remnants, galaxies, and the intracluster medium of galaxy clusters. Spectroscopic diagnostics for electron temperature, electron density, and elemental abundances rely on accurate charge state distribution calculations. The ionization structure is determined by the balance between EII and electron–ion recombination. For most objects, ions are found at an electron temperature where only electron impact single ionization (EISI) is important. But in some systems sudden heating can generate enough high energy electrons for electron impact double ionization (EIDI) to be important (Müller [1986]). Accurate data for all these processes are needed to reliably interpret astrophysical spectra (Dere [2007]).

A major limitation of much existing experimental EII data has been the inability to perform measurements on beams of purely ground state ions. Most experimental arrangements have worked with ion beams that contain an unknown fraction of metastables. Since the ionization cross section from the metastable levels usually differs from that of the ground level, disentangling the data is not possible and the results of such experiments are ambiguous.

Here we describe measurements of EII for Cl-like Fe^{9+} and S-like Fe^{10+}. Previous measurements of these ions as well as for isoelectronic ions have suffered from large unknown metastable fractions in the ion beams used, limiting their usefulness for benchmarking theory (Gregory et al. [1986]; Stenke et al. [1999]; Dere [2007] and references therein). We resolved this problem by

using an ion storage ring to produce nearly pure ground state ion beams. Storing the ions for several seconds before data are collected allows essentially all of the metastables to radiatively relax to the ground state. Our measurements are thereby able to provide accurate tests for theoretical models.

The EISI cross section for both Fe^{9+} and Fe^{10+} were measured from below the ionization threshold up to ≈ 1800 eV. Over this energy range various ionization channels are possible. For Fe^{9+} direct ionization can occur through

$$
e^- + Fe^{9+}(2s^2\,2p^6\,3s^2\,3p^5)
$$
$$
\rightarrow
\begin{cases}
Fe^{10+}(2s^2\,2p^6\,3s^2\,3p^4) + 2e^- \\
Fe^{10+}(2s^2\,2p^6\,3s\,3p^5) + 2e^- \\
Fe^{10+}(2s^2\,2p^5\,3s^2\,3p^5) + 2e^- \\
Fe^{10+}(2s^1\,2p^6\,3s^2\,3p^5) + 2e^-
\end{cases} . \quad (1)
$$

The ionization thresholds for the $3p$ and $3s$ electrons are 262.10 eV and 297.26 eV, respectively (Ralchenko et al. [2011]). Direct ionization of the $2p$ and $2s$ electrons can occur at 1000 eV and 1129 eV (Kaastra & Mewe [1993]), but the resulting excited states decay through autoionization of a second electron more than 90% of the time, resulting in a net double ionization rather than single ionization (Kaastra & Mewe [1993]). There are also a number of excitation-autoionization (EA) channels that can be important. Starting at the 262.10 eV ionization threshold of a $3p$ electron, it is also possible to excite a $3s$ electron to a level lying in the continuum of the initial system. This can then relax via autoionization. At energies above about 650 eV, EA can also occur via excitation from the $n = 2$ shell (Arnaud & Raymond [1992]).

Double ionization of Fe^{9+} forming Fe^{11+} was measured from below the direct double ionization threshold of 552.35 eV up to 3000 eV. As discussed above, single ionization of an $n = 2$ electron results in an excited state that usually decays through autoionization, i.e., ejection of a second electron. For Fe^{9+} the threshold for this process is 1000 eV (Kaastra & Mewe 1993) and it is expected to dominate the double ionization cross section for highly charged ions (Müller & Frodl 1980).

For Fe^{10+} the direct ionization channels are

$$e^- + Fe^{10+}(2s^2\,2p^6\,3s^2\,3p^4)$$
$$\rightarrow \begin{cases} Fe^{11+}(2s^2\,2p^6\,3s^2\,3p^3) + 2e^- \\ Fe^{11+}(2s^2\,2p^6\,3s\,3p^4) + 2e^- \\ Fe^{11+}(2s^2\,2p^5\,3s^2\,3p^4) + 2e^- \\ Fe^{11+}(2s^1\,2p^6\,3s^2\,3p^4) + 2e^- \end{cases}. \qquad (2)$$

The thresholds for direct ionization of $3p$, $3s$, $2p$, and $2s$ electrons are 290.25 eV, 324.27 eV, 1036 eV, and 1164 eV, respectively (Kaastra & Mewe 1993; Ralchenko et al. 2011). However, the states resulting from direct ionization of $n = 2$ electrons decay more than 90% of the time by autoionizing a second electron (Kaastra & Mewe 1993). EA can also occur through channels similar to those in Fe^{9+}.

2. EXPERIMENTAL METHOD AND ANALYSIS

Measurements were carried out using the TSR heavy ion storage ring at the Max-Planck-Institut für Kernphysik in Heidelberg, Germany. The procedures used here closely follow those described by Linkemann et al. (1995) and Hahn et al. (2010, 2011a, 2011b, 2012).

First a beam of 94 MeV $^{56}Fe^{9+}$ ions or 116 MeV $^{56}Fe^{10+}$ ions was injected into TSR where it was merged with two electron beam devices named the Cooler and the Target. Each is located in different sections of the ring. Initially both beams were set so that the electron velocity was close to the average ion velocity. Elastic electron collisions with the ions brought the ions to the electron velocity and reduced their energy spread (i.e., electron cooling; Poth 1990). The initial cooling cycle lasted two seconds, during which time metastable levels in the ion beam could radiatively decay.

We modeled the level populations versus time in order to estimate the metastable fraction remaining in the beam after the cooling cycle, as described in more detail in Hahn et al. (2011b) and Lestinsky et al. (2012). For this model the assumed initial Boltzmann distribution of levels was evolved using the radiative decay rates of Ralchenko et al. (2011). The calculation showed that essentially all metastables were removed from the Fe^{9+} beam following the cooling cycle. For Fe^{10+}, the metastable fraction after two seconds was due mainly to the $3s^2\,3p^4\,^3P_0$ level with a population of less than about 3%. When averaged over a typical ≈ 50 s data acquisition period, the metastable fraction for Fe^{10+} was $\lesssim 0.01\%$. For comparison, the $1/e$ lifetime of the stored ion beam was about 30 s for Fe^{9+} and about 50 s for Fe^{10+}.

Next, the Cooler electron energy was scanned in order to study electron–ion collisions at different energies. During this time the Target electron beam energy was maintained at cooling. Ions that underwent ionization while traveling through the Cooler electron beam were directed by a dipole magnet onto a charged particle detector. Between each energy step the count rate was also measured at a fixed reference energy in order to determine the background rate due to electron stripping off the residual

Table 1
Sources of Uncertainty

Source	Estimated 1σ Uncertainty	
	Fe^{9+}	Fe^{10+}
Counting statistics	1%	1%
Detector efficiency	3%	3%
Ion current measurement	8%	8%
Electron density	3%	3%
Pressure fluctuations[a]	2% (4%)	...
Quadrature sum	9% (10%)	9%

Notes. [a] For Fe^{9+} the 2% uncertainty is for $E < 941$ eV for EISI and $E < 1320$ eV for EIDI. The 4% uncertainty applies to higher energies. For Fe^{10+} no systematic pressure fluctuations were observed.

gas. At high energies the limited dynamic range of the electron beam power supply prevented us from setting a reference point below the EII threshold. In such cases, the EII contribution to the reference rate was assessed using the EII cross section derived from lower energy scans, allowing the stripping background rate to be determined. This procedure was necessary for Fe^{9+} at energies $E > 941$ eV for single ionization and $E > 1320$ eV for double ionization, and for Fe^{10+} at $E > 900$ eV for single ionization.

The EII cross section σ_I was calculated by subtracting the background count rate from the measured count rate, then dividing by the electron density and the number of stored ions in the interaction region. The detector efficiency introduces an uncertainty of about 3% on the measured count rates (Rinn et al. 1982). All uncertainties throughout are quoted at an estimated 1σ confidence level. The electron density was determined from the measured current and known geometry of the electron beam. The uncertainty of the electron density was estimated to be about 3% (Lestinsky et al. 2009). The ion current, and hence the number of stored ions, was measured using a beam profile monitor (BPM; Hochadel et al. 1994). The BPM calibration depends on the residual gas pressure and electronic drifts and tends to vary on a timescale of several hours. It was periodically cross calibrated with a DC transformer (Unser 1981) using currents up to 86 μA as described by Hahn et al. (2011b). The DC transformer could not be used directly in the data analysis because it is not sufficiently sensitive to the small currents of $\sim$1–10 μA that were present during measurement. Based on the uncertainty of the calibration, we estimate that the 1σ uncertainty of σ_I due to the ion current measurement is about $\pm 8\%$.

Following Hahn et al. (2010), we corrected σ_I for pressure fluctuations, which are a function of the electron beam energy and change the background rate. For Fe^{9+} the correction was about $(4 \pm 2)\%$. For Fe^{10+} we could not identify any significant systematic relationship between beam energy and pressure and so no correction was performed. The correction can only be applied when the reference point is below the EII threshold so there is an additional $\approx 4\%$ uncertainty on the Fe^{9+} EISI cross section above 941 eV and on the Fe^{9+} EIDI cross section above 1320 eV. Table 1 summarizes the various experimental uncertainties.

3. RESULTS AND DISCUSSION

3.1. Single Ionization

Figures 1 and 2 show the EISI cross sections for Fe^{9+} forming Fe^{10+} and Fe^{10+} forming Fe^{11+}, respectively. Samples of the
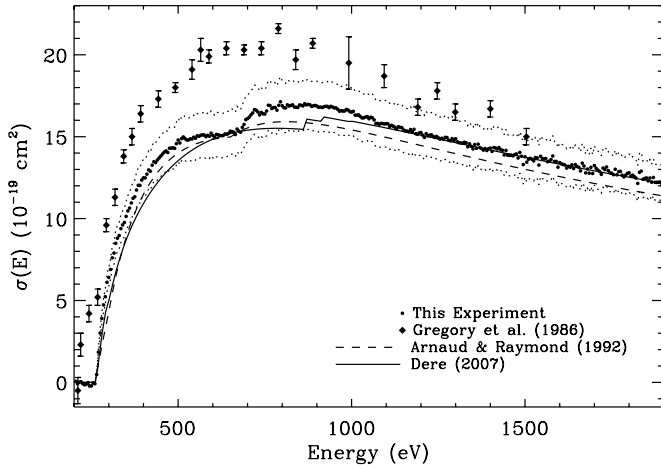
Figure 1. EII cross section for Fe^{9+} forming Fe^{10+} (circles). The 1σ systematic uncertainties are illustrated by the dotted curves. The 1% statistical uncertainties are generally smaller than the symbol size and are not plotted. The diamonds show the experimental results of Gregory et al. (1986). The theoretical cross sections given by Arnaud & Raymond (1992) and Dere (2007) are shown by the dashed and solid curves, respectively.
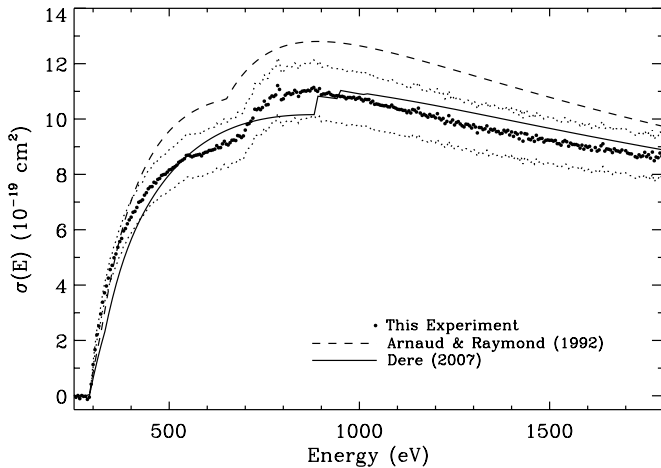

Figure 2. Same as Figure 1, but for Fe^{10+} forming Fe^{11+}.

cross-section data are given in Tables 2 and 3. These data are available in their entirety in the electronic edition of this journal. The dotted curves in Figures 1 and 2 illustrate the 1σ systematic uncertainties. The errors due to counting statistics are less than 1%, which is generally smaller than the symbol size used in the plots. Figure 1 also presents the cross-section measurement by Gregory et al. (1986), which was affected by a large unknown metastable ion fraction in the beam. Their cross section is about 30% larger than the present measurement and demonstrates the effect of metastable ions on the EII measurements.

Two theoretical cross sections are also shown in Figures 1 and 2. The dashed curves show the recommended cross section of Arnaud & Raymond (1992), which was used in their collisional ionization balance calculations and those of Mazzotta et al. (1998). The Arnaud & Raymond (1992) cross section is based on the theoretical calculations of Younger (1983) for direct ionization and Pindzola et al. (1986) for EA. The solid curves illustrate the cross section calculated by Dere (2007). The cross section of Arnaud & Raymond (1992) lies within the experimental uncertainties for Fe^{9+}, but is significantly larger than the measured result for Fe^{10+}. The reason for this is not clear to us. The cross sections calculated by Dere (2007) for

Table 2
Fe^{9+} Single Ionization Cross Section

E (eV)	σ_I (cm^2)	Statistical Error
250.0	$-2.1237E-20$	$1.3112E-20$
400.0	$1.2489E-18$	$1.2462E-20$
550.0	$1.4904E-18$	$6.4683E-21$
700.0	$1.6104E-18$	$7.1986E-21$
850.0	$1.6935E-18$	$4.9529E-21$
1000.0	$1.6499E-18$	$5.9026E-21$
1150.0	$1.5414E-18$	$1.1248E-20$

Note. In the electronic edition, data are given over the range 205–1900 eV in 5 eV intervals.

(This table is available in its entirety in a machine-readable form in the online journal. A portion is shown here for guidance regarding its form and content.)

Table 3
Fe^{10+} Single Ionization Cross Section

E (eV)	σ_I (cm^2)	Statistical Error
300.0	$1.1274E-19$	$4.8542E-21$
450.0	$7.5490E-19$	$4.6503E-21$
600.0	$8.8076E-19$	$2.8859E-21$
750.0	$1.0645E-18$	$2.3292E-21$
900.0	$1.0877E-18$	$4.2591E-21$
1050.0	$1.0529E-18$	$3.2853E-21$
1200.0	$1.0043E-18$	$9.6823E-21$

Note. In the electronic edition, data are given over the range 250–1850 eV in 5 eV intervals.

(This table is available in its entirety in a machine-readable form in the online journal. A portion is shown here for guidance regarding its form and content.)

both Fe^{9+} and Fe^{10+} fall within the experimental uncertainties at most energies.

Despite the good agreement in magnitude between the Dere (2007) results and our measurements, several significant discrepancies can readily be seen which are most likely due to the treatment of EA in the calculations. Near threshold, the experimental cross section rises more rapidly than do the theoretical cross sections of Dere, especially for the case of Fe^{10+}. This has been observed previously for other ions with a $3s^2 3p^q$ configuration (Hahn et al. 2011a, 2011b). It is probably due to collisional excitation of a $3s$ electron to an autoionizing state. Dere (2007) included in the Fe^{9+} calculations what appear to be the first three EA channels ($n = 3 \rightarrow 6$, $n = 3 \rightarrow 7$, and $n = 3 \rightarrow 8$ transitions), but did not include any such channels for Fe^{10+}. Theory and experiment near threshold do appear to agree slightly better for Fe^{9+} than for Fe^{10+}, but a significant deviation remains. This might be due to neglecting channels for excitation to beyond $n = 8$.

The experimental results also show a step in the cross section at about 650 eV, corresponding to the energy threshold for EA due to $n = 2 \rightarrow 3$ excitations. This process is also included in the Arnaud & Raymond (1992) cross section, although in the case of Fe^{9+} the magnitude is somewhat smaller than we find experimentally. No step appears in the Dere (2007) cross section because $n = 2 \rightarrow 3$ EA is not included in the calculations. Conversely, Dere (2007) does include $n = 2 \rightarrow 4$ and $n = 2 \rightarrow 5$ EA, but these contributions are not observed experimentally. Similar discrepancies with the Dere (2007) results have been found previously for Fe^{11+} (Hahn et al. 2011a)
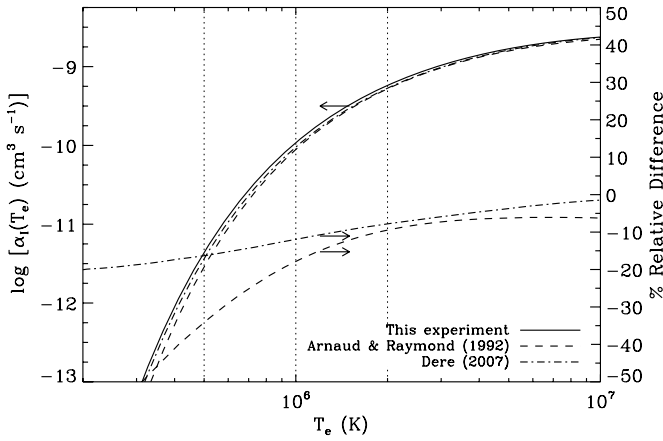
Figure 3. Plasma rate coefficient for Fe^{9+} forming Fe^{10+}. The experimental results are shown by the solid curve and compared to the values from Arnaud & Raymond (1992, dashed curve) and Dere (2007, dash-dotted curve). These can be read off the left axis. The relative difference between these and the present results are also indicated and can be read off the right axis. The vertical dotted lines illustrate the temperature range where Fe^{9+} is greater than 1% abundant in collisional ionization equilibrium with the center line indicating the temperature at which the Fe^{9+} abundance peaks (Bryans et al. 2009).
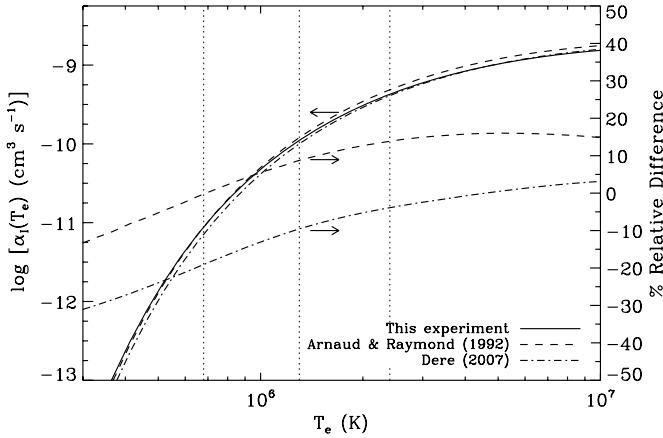

Figure 4. Same as Figure 3, but for Fe^{10+} forming Fe^{11+}.

and Fe^{12+} (Hahn et al. 2011b). Possible explanations are that their calculations underestimate the branching ratio for radiative stabilization (resulting in no net ionization), underestimate the branching ratio for auto-double-ionization (resulting in a net double ionization), or some combination thereof.

We have derived plasma ionization rate coefficients $\alpha_I(T_e)$ from the measured cross sections using the methods described in Hahn et al. (2011a). Figures 3 and 4 show the results compared to the rate coefficients from Arnaud & Raymond (1992) and Dere (2007). In collisional ionization equilibrium Fe^{9+} is greater than 1% abundant from 5.0×10^5 K to 2.0×10^6 K with a peak abundance at 1.1×10^6 K. Fe^{10+} is greater than 1% abundant from 6.8×10^5 K to 2.4×10^6 K and peaks at 1.3×10^6 K (Bryans et al. 2009). These temperatures are indicated by the dotted vertical lines in Figures 3 and 4. At temperatures where each ion is abundant, the rate coefficients of Arnaud & Raymond (1992) differ from our experimental result for Fe^{9+} by less than $\approx 34\%$ and for Fe^{10+} by less than $\approx 14\%$. Compared to the experimental values, the Dere (2007) rate coefficients for Fe^{9+} are within $\approx 16\%$ and those for Fe^{10+} are within $\approx 19\%$.

Table 4 presents coefficients of a fifth-order polynomial fit for the scaled rate coefficient ρ, which can be used to reproduce
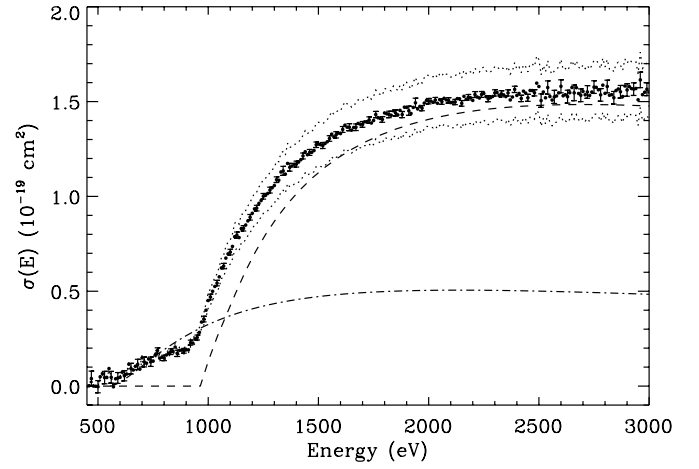

Figure 5. Double ionization cross section for Fe^{9+} forming Fe^{11+}. Error bars on selected points indicate the 1σ statistical uncertainty and the dotted curves show the 1σ systematic uncertainty. The dash-dotted curve shows a semiempirical prediction for the direct double ionization cross section. The dashed curve is an estimate for the double ionization cross section due to direct ionization of an L-shell electron followed by autoionization of the resulting excited state. See the text for details on each calculation.

Table 4
Fifth-order Polynomial Fitting Parameters to Reproduce the Scaled Ionization Rate Coefficient $\rho = 10^{-6} \sum_{i=0}^{i=5} a_i x^i$ (see Equations (4) and (5))

i	Fe^{9+} a_i	Fe^{10+} a_i
0	28.4757	18.3490
1	−76.3317	−20.2960
2	280.844	16.0389
3	−506.699	122.420
4	465.127	−247.492
5	−183.273	124.888

the experimental plasma rate coefficients. The tabulated values should be multiplied by a factor of 10^{-6} to obtain a rate coefficient in units of $cm^3\,s^{-1}$. Note that this factor should also be applied to the fitting coefficients of Hahn et al. (2011a, 2011b). The fit was performed on the data after applying the scaling of Dere (2007). The scaled rate coefficient ρ as a function of scaled temperature x,

$$x = 1 - \frac{\ln 2}{\ln(t+2)} \qquad (3)$$

is related to $\alpha_I(T_e)$ through

$$T_e = \frac{E_0}{k_B}\left[\exp\left(\frac{\ln 2}{1-x}\right) - 2\right] \qquad (4)$$

and

$$\alpha_I(T_e) = t^{-1/2} E_0^{-3/2} E_1(1/t)\rho, \qquad (5)$$

where E_0 is the ionization threshold (262.10 eV for Fe^{9+} and 290.25 eV for Fe^{10+}), k_B is the Boltzmann constant, $t = k_B T_e / E_0$, and $E_1(1/t)$ is the first exponential integral. These fits reproduce the experimental rate coefficients to about 1% accuracy or better for $T_e = 1 \times 10^5$–1×10^8 K.

3.2. Double Ionization

Figure 5 shows the measured double ionization cross section for Fe^{9+} with error bars on selected points to indicate the statistical uncertainty and dotted curves to illustrate the systematic

Table 5
Fe^{9+} Double Ionization Cross Section

E (eV)	σ_I (cm^2)	Statistical Error
500.0	$-3.3830E-22$	$3.2182E-21$
700.0	$1.4894E-20$	$2.5496E-21$
900.0	$1.9105E-20$	$1.2356E-21$
1100.0	$7.0631E-20$	$1.4951E-21$
1300.0	$1.0573E-19$	$1.5134E-21$
1500.0	$1.2763E-19$	$1.6696E-21$
1700.0	$1.3798E-19$	$1.5233E-21$
1900.0	$1.4693E-19$	$2.3853E-21$

Note. In the electronic edition, the range 450–3000 eV in 10 eV intervals is published.

(This table is available in its entirety in a machine-readable form in the online journal. A portion is shown here for guidance regarding its form and content.)

uncertainty. Table 5 presents a sample of the cross-section data. This table appears in its entirety in the electronic edition of this journal. From the double ionization threshold of 552.35 eV to about 1000 eV the EIDI cross section is due to direct double ionization and excitation double autoionization, although the resolution of the measurement is insufficient to resolve individual autoionization channels. In this energy range we can compare the experimental result to the semiempirical prediction for direct double ionization of Shevelko & Tawara (1995) and Bélenger et al. (1997). We find that the semiempirical formula rises faster than the measurement, as was also found for Cl-like Ti^{5+}, by Hartenfeller et al. (1998a). However, their single ionization measurements showed that their Ti^{5+} beam contained a large metastable fraction (Hartenfeller et al. 1998b); so the present measurements remove this ambiguity as a possible explanation for the observed differences.

We also see a rapid rise in the EIDI cross section at $\approx$1000 eV, due to direct ionization of an L-shell electron followed by autoionization when the hole is filled in. The dashed curve illustrates the expected double ionization cross section due to this process. It was obtained by calculating the $n = 2$ single ionization cross section using the LANL Atomic physics code (Magee et al. 1995) and scaling that by the Auger yields given by Kaastra & Mewe (1993). This process can account for more than 50% of the total measured cross section above about 1060 eV. This is comparable to what has been observed for other Cl-like ions (Hartenfeller et al. 1998a; Cherkani-Hassani et al. 2001).

4. SUMMARY

We have measured the ground state cross sections for EISI of Fe^{9+} and Fe^{10+} and EIDI of Fe^{9+}. In terms of the overall magnitude of the cross section, we find that the single ionization measurements are in reasonably good agreement with theoretical cross sections currently used in ionization balance calculations. However, we observe clear discrepancies between the experiment and theory. We attribute this to an incomplete treatment of EA in the calculations. Existing theoretical results have

neglected $3s$ EA, which is an important ionization channel near threshold. They have also, in some cases, neglected $n = 2 \rightarrow 3$ excitations, which appear to be the dominant EA channel above $\sim$650 eV. For either ion, we do not find the EA contributions from $n = 2 \rightarrow 4$ and $n = 2 \rightarrow 5$ transitions that are predicted by theory. This may be due to inaccurate theoretical branching ratios for radiative stabilization or auto-double-ionization versus autoionization of a single electron. Thus, our experimental benchmarks have identified several areas in which the calculations can be improved in order to produce more accurate EII data. For double ionization we find that the cross sections are dominated by single ionization of an $n = 2$ electron producing a state that relaxes through autoionization. Our EIDI measurements are also consistent with the results for other Cl-like ions.

REFERENCES

Arnaud, M., & Raymond, J. 1992, ApJ, 398, 394
Bélenger, C., Defrance, P., Salzborn, E., et al. 1997, J. Phys. B, 30, 2667
Bryans, P., Landi, E., & Savin, D. W. 2009, ApJ, 691, 1540
Cherkani-Hassani, S., Khouilid, M., & Defrance, P. 2001, Phys. Scr. T, 92, 287
Dere, K. P. 2007, A&A, 466, 771
Gregory, D. C., Meyer, F. W., Müller, A., & Defrance, P. 1986, Phys. Rev. A, 34, 3657
Hahn, M., Bernhardt, D., Grieser, M., et al. 2011a, ApJ, 729, 76
Hahn, M., Bernhardt, D., Grieser, M., et al. 2012, Phys. Rev. A, 85, 042713
Hahn, M., Bernhardt, D., Lestinsky, M., et al. 2010, ApJ, 712, 1166
Hahn, M., Grieser, M., Krantz, C., et al. 2011b, ApJ, 735, 105
Hartenfeller, U., Aichele, K., Hathiramani, D., et al. 1998a, J. Phys. B, 31, 3013
Hartenfeller, U., Aichele, K., Hathiramani, D., et al. 1998b, J. Phys. B, 31, 2999
Hochadel, B., Albrecht, F., Grieser, M., et al. 1994, Nucl. Instrum. Methods A, 343, 401
Kaastra, J. S., & Mewe, R. 1993, A&AS, 97, 443
Lestinsky, M., Badnell, N. R., Bernhardt, D., et al. 2009, ApJ, 698, 648
Lestinsky, M., Badnell, N. R., Bernhardt, D., et al. 2012, ApJ, 758, 40
Linkemann, J., Müller, A., Kenntner, J., et al. 1995, Phys. Rev. Lett., 74, 4173
Magee, N. H., Abdallah, J., Jr., Clark, R. E. H., et al. 1995, in ASP Conf. Ser. 78, Astrophysical Applications of Powerful New Databases, ed. S. J. Adelman & W. L. Wiese (San Francisco, CA: ASP), 51
Mazzotta, P., Mazzitelli, G., Colafrancesco, S., & Vittorio, N. 1998, A&AS, 133, 403
Müller, A. 1986, Phys. Lett. A, 113, 415
Müller, A., & Frodl, R. 1980, Phys. Rev. Lett., 44, 29
Pindzola, M. S., Griffin, D. C., & Bottcher, C. 1986, Phys. Rev. A, 35, 3668
Poth, H. 1990, Phys. Rep., 196, 135
Ralchenko, Y., Kramida, A., Reader, J., & NIST ASD Team. 2011, NIST Atomic Spectra Database, National Institute of Standards and Technology, http://physics.nist.gov/asd
Rinn, K., Müller, A., Eichenauer, H., & Salzborn, E. 1982, Rev. Sci. Instrum., 53, 829
Shevelko, V. P., & Tawara, H. 1995, J. Phys. B, 28, L598
Stenke, M., Aichele, K., Hartenfeller, U., et al. 1999, J. Phys. B, 32, 3627
Unser, K. 1981, IEEE Trans. Nucl. Sci., 28, 2344
Younger, S. M. 1983, J. Quant. Spectrosc. Radiat. Transfer, 29, 61